Kinetics of the Decomposition of Hydrogen Sulfide in a Dielectric Barrier Discharge Reactor

ARTICLE *in* CHEMICAL ENGINEERING & TECHNOLOGY · NOVEMBER 2012

Impact Factor: 2.44 · DOI: 10.1002/ceat.201200134

Enakonda Linga Reddy[1]
Jaya Karuppiah[1]
Albert Renken[2]
Lioubov Kiwi-Minsker[2]
Challapalli Subrahmanyam[1]

[1] Indian Institute of Technology Hyderabad, Department of Chemistry, Hyderabad, India.

[2] Ecole Polytechnique Fédérale de Lausanne (GGRC-EPFL), Lausanne, Switzerland.

Research Article

Kinetics of the Decomposition of Hydrogen Sulfide in a Dielectric Barrier Discharge Reactor

Kinetics of hydrogen sulfide (H_2S) decomposition to hydrogen and sulfur was investigated in a nonthermal plasma dielectric barrier discharge (NTP-DBD) reactor operated under ambient conditions. The reactions were carried out with a fixed flow rate and varying inlet concentration. The results indicated that the dissociation of H_2S into H_2 and S may be initiated by excitation of the carrier gas argon. A reaction rate model based on a Langmuir Hinshelwood/Michaelis-Menten model was proposed. The formal reaction order approaches zero at high H_2S concentrations. The parameters of the kinetic model were found to be dependent on the power input.

Keywords: Desulfurization, Dielectric barrier discharge reactor, Hydrogen sulfide, Kinetics

Received: March 04, 2012; *revised:* July 23, 2012; *accepted:* July 31, 2012

DOI: 10.1002/ceat.201200134

1 Introduction

Hydrogen sulfide (H_2S) is produced in large amounts from hydrocarbon upgrading processes associated with petroleum refining and natural gas industries. It is treated normally by the conventional Claus process, in which sulfur is only recovered and H_2 converted in the form of water [1]. Alternative methods also available for flue gas cleaning like nitriding processes are based on catalytic dissociation of ammonia [2]. Nonthermal plasma (NTP) is an attractive alternative energy source for unconventional reactions that demand severe operating conditions [3]. Dielectric barrier discharge (DBD) belongs to the NTP technologies that utilize high electrical voltage between two electrodes separated by a dielectric material. DBD produces microdischarges through the growth of electron avalanches formed by electron collision ionization events [4]. NTP decomposition of H_2S towards hydrogen and sulfur has become a subject of extensive investigations for the effective utilization of H_2S, which is produced as an unavoidable by-product in processes like heavy oil dehydrodesulfurization and coal gasification. It may also be present in natural gas [1]. The major advantage of the direct decomposition of H_2S compared to the conventional Claus process is the production of hydrogen along with sulfur. Hydrogen is a valuable product used as raw material in the chemical industry and as feedstock in fuel cells for clean energy production [1, 5].

Only little work was reported on the decomposition of H_2S by NTP, whereas kinetics has been studied for thermal or catalytic H_2S decomposition [6–11]. Nicholas et al. determined the kinetics and proposed a mechanism of the decomposition of H_2S, CH_3SH, and $(CH_3)_2S$ in a radio-frequency pulse discharge. The study was carried out with short duration pulses and gas pressures in the range of 13–267 Pa [12]. The mechanism of H_2S decomposition reactions in NTP pulsed corona discharge reactor was investigated by Zhao et al. [13]. The authors suggested that H_2S decomposition is initiated by excitation of the carrier gas molecules [13]. Here, a kinetic model of the H_2S decomposition in a DBD reactor is elucidated and model parameters are estimated to describe the rate of reactions involved in the decomposition.

2 Materials and Methods

Details of the DBD reactor are reported elsewhere [14, 15]. A schematic presentation is given in Fig. 1. The dielectric discharge was generated in a cylindrical quartz tube with an inner diameter of 19 mm. Silver paste painted on the outside of the quartz tube over a length of 10 cm was used as outer electrode, whereas a stainless-steel rod functioned as inner electrode. The diameter of the inner electrode was 12 mm. A high-voltage alternating current in the range of 12–22 kV and a frequency of 50 Hz were applied. The voltage of the system was measured by means of an oscilloscope (Tektronix, TDS 2014 B) with a 1000:1 high-voltage probe (Agilent 34136A HV). The charge Q

Correspondence: Dr. C. Subrahmanyam (csubbu@iith.ac.in), Indian Institute of Technology Hyderabad, Department of Chemistry, Hyderabad-502205, India.

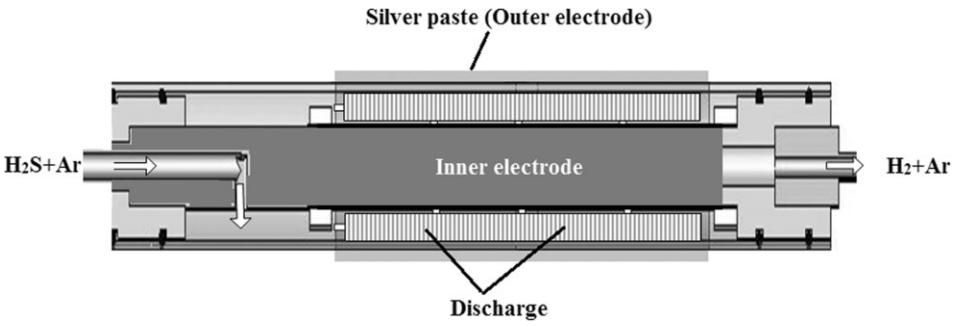

Figure 1. Schematic presentation of a dielectric barrier discharge reactor.

was determined by recording the voltage across a capacitor-connected series to the ground electrode. The H_2S gas diluted in argon (Ar) was introduced into the system through a Teflon tube. The H_2S concentration at the outlet was measured with a gas chromatograph (Shimadzu GC-2014) equipped with a packed column and a TCD detector. The conversion of H_2S at each voltage was determined after 30 min time-on-stream. The hydrogen concentration was further confirmed with a hydrogen gas analyzer (Siemens, calomat 6E). A V-Q Lissajous method was used to determine the discharge power in the plasma reactor. The area of the Lissajous figure characterizes the energy dissipated in the discharge during one period of the voltage [14–18].

3 Results and Discussion

3.1 H_2S Decomposition in a DBD Plasma Reactor

The experimentally obtained H_2S conversions as function of the concentration (5–25 vol % in Ar) and power in a DBD reactor with a discharge gap of 3.5 mm are presented in Fig. 2. The interesting observation is that, in the present study, hydrogen and sulfur are the only products. This highlights the advantage of the plasma technique compared to the conventional Claus process, where hydrogen is converted into water [1]. The selectivity to hydrogen was always 100 %, as confirmed by gas chromatographic analysis. As seen from Fig. 2, H_2S conversion increases linearly with increasing input power at any concentration, and conversion decreases with increasing inlet concentration. For example, for 5 vol % the conversion was 24 % at 0.65 W and increases to 44 % at 0.98 W, whereas for an inlet concentration of 25 vol %, the conversion varied between 4 % and 13 % at 0.2 and 1.4 W, respectively. These results suggest a formal reaction order lower than 1.

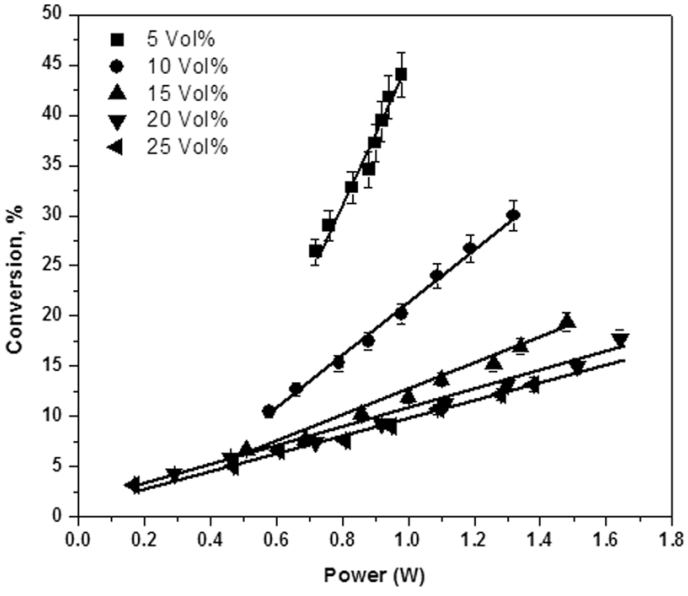

Figure 2. Conversion as a function of power for different H_2S inlet concentrations.

3.2 Influence of a Catalyst on H_2S Decomposition

The effect of a catalyst on H_2S conversion is of great interest in oil industry. In our earlier experiments, different catalysts like Al_2O_3, MoO_x/Al_2O_3, CoO_x/Al_2O_3, and NiO/Al_2O_3 were studied for H_2S decomposition in combination with NTP, where MoO_x/Al_2O_3 provided the best conversion [19]. Here, 500 mg of 3, 5, and 7 wt % of MoO_x/Al_2O_3 was dispersed into quartz wool and placed inside the discharge zone. The H_2S inlet concentration was fixed at 5 vol %, diluted in Ar. Fig. 3 indicates that 5 wt % MoO_x/Al_2O_3 resulted in better conversion than 3 wt % and 7 wt %. The reason may be that 3 wt % catalyst may become quickly poisoned due to sulfur deposition, whereas 7 wt % MoO_x catalyst may change the discharge behavior due to the high oxide content. At an applied power of ~ 1 W, 5 wt % MoO_x/Al_2O_3 led to 52 % conversion that decreased to 25 % with decreasing the power to ~ 0.7 W. Under the same experimental conditions (at ~ 0.7 W), 3 wt % and 7 wt % catalysts resulted in only 24 % and 23 % conversion, respectively. With decreasing the input power from ~ 1 W to ~ 0.7 W (Fig. 3), the conversion decreased drastically and the catalyst has no effect after 1 h. This decrease may be due to deactivation of the catalyst by sulfur deposition. The sulfur deposited on the reactor walls was periodically removed by heating the reactor to 430 K.

3.3 Mechanism of H_2S Decomposition

Understanding the formation of reactive species and their reaction pathways is essential to optimize the NTP pro-

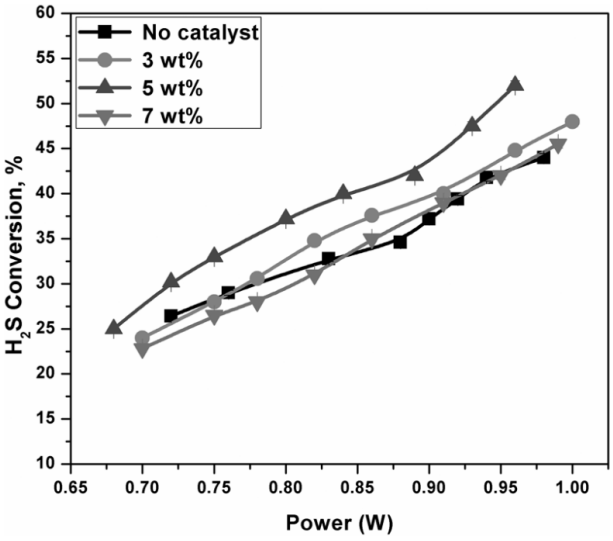

Figure 3. Conversion of H_2S with respect to power (W) over different wt % of MoO_x/Al_2O_3 catalyst at 5 vol % H_2S initial concentration, 50 Hz frequency, and 150 mL min^{-1} flow rate.

cessing for H_2 production. It is known that plasma is composed of molecules, electrons, atoms, radicals, and ions, and that the multiple active species produced in NTP through electron collision reactions with the background gas may lead to complex reaction mechanisms. The mechanism of H_2S decomposition in plasma and the active species involved in H_2S decomposition is not clear. Zhao et al. proposed that the concentration of radicals and excited states formed by electron collisions was around two to four orders of magnitude higher than that of the ions. They reported that for Ar + H_2S gas mixtures the main active species was metastable Ar and that charge transfer reactions of cations only contribute negligibly to H_2S conversion in NTP [13]. The research group demonstrated that there are 14 active excited states of Ar formed, where the lowest energy excited state, $Ar(^3p_2)$, may contribute to the dissociation of H_2S [20]. Finally, two different dissociation mechanisms were proposed to be the major pathway for H_2S conversion.

Direct electron collisions with H_2S leading to dissociation:

$$e + H_2S \rightarrow HS^{\bullet} + H^{\bullet} + e \quad (1)$$

Direct electron collisions with Ar forming $Ar(^3p_2)$:

$$e + Ar \rightarrow Ar(^3p_2) + e \quad (2)$$

In the case of a high H_2S inlet concentration, direct electron collision with H_2S may be favorable and reaction (1) is more likely to happen as the excitation energy of H_2S is far less than the one of Ar. Direct electron collisions with Ar, reaction (2), was proposed to be dominant at low H_2S inlet concentration, which may be due to the fact that more Ar molecules are present in the gas, so that the probability for an electron to collide with Ar is much higher than with H_2S [13]. In that case, reaction (2) may be considered as the driving step and the following reaction is proposed to follow reaction (2):

$$Ar(^3p_2) + H_2S \rightarrow Ar + H^{\bullet} + HS^{\bullet} \quad (3)$$

Reactions (1) and (3) lead to the H_2 and S formation by the following probable reaction steps:

$$HS^{\bullet} + H^{\bullet} \rightarrow H_2 + 1/2S_2 \quad (4)$$

$$2H^{\bullet} \rightarrow H_2 \quad (5)$$

$$2HS^{\bullet} \rightarrow H_2 + S_2 \quad (6)$$

3.4 Kinetic Study

The kinetics of the H_2S decomposition reaction in NTP aimed at defining a rate expression that allows modeling the experimental data. To analyze the kinetics of the decomposition reaction, the conversion was followed by varying the concentration and power at a frequency of 50 Hz and a discharge gap of 3.5 mm. This allowed the plot $X = f(P)$ for different inlet concentrations, which is presented in Fig. 4. In conclusion, two parameters should be considered to establish the reaction rate, namely the inlet concentration and the power. In addition, the conversion was found to depend linearly on the applied power. One may see that for high inlet concentrations the conversion is low and increases only slightly with the input power.

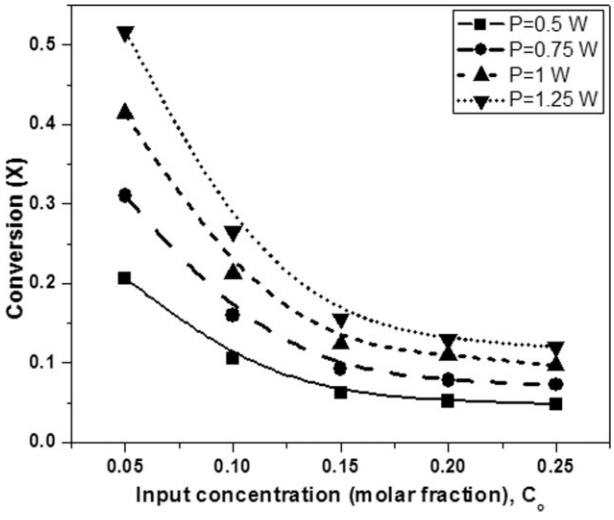

Figure 4. Linearized equation of the conversion versus the H_2S inlet concentration where the parameters *a* and *b* have been adjusted to fit to the experimental points, $X = f(H_2S)_{in}$.

The mechanism of H_2S decomposition is composed of multiple complex reactions as discussed above. Therefore, a kinetic model for the H_2S decomposition reaction, based on Langmuir-Hinshelwood/Michaelis-Menten kinetics, is proposed. It is supposed that the reaction order could increase from 0 to 1 when the inlet concentration is decreased. Such a behavior is known for homogeneously and heterogeneously catalyzed reactions, where the order decreases from first to zero with increasing reactant concentrations. A similar equation was adopted in this study:

$$r = -R = \frac{aC_{H_2S}}{b+C_{H_2S}} \quad (7)$$

where R is the intrinsic reaction rate, C_{H2S} is the local H_2S concentration in the reactor, and a and b are model parameters.

$$-R = \frac{aC_{H_2S}}{b+C_{H_2S}} = C_0\frac{dX}{d\tau} \quad (8)$$

Integration of Eq. (7) leads to a relatively simple relation between conversion (X) and inlet concentration (C_0) for a given residence time (τ):

$$C_0\int_0^X \frac{b+C_0(1-X)}{aC_0(1-X)}dX = \int_0^\tau d\tau' \quad (9)$$

$$\tau = \frac{C_0}{a}X - \frac{b}{a}\ln(1-X)$$

$$a\tau = C_0X - b\ln(1-X)$$

$$C_0X = a\tau + b\ln(1-X)$$

$$C_0 = \frac{a\tau}{X} + \frac{b}{X}\ln(1-X) \quad (10)$$

The parameters a and b were determined by fitting Eq. (10) to the experimental data $X=f[C(H_2S)_{in}]$, as seen in Fig. 4. A relatively good fit to the experimental data has been obtained. Based on these results one can conclude that the rate expression presents an adequate kinetic model to describe the experimental results. The parameters a and b were plotted as a function of power that confirms a linear increase of parameter a with power, as observed in Fig. 5.

For parameter b, as illustrated in Fig. 6, a hyperbolic function with power is found. It may be concluded that parameter a can be seen as the apparent rate constant (k_{app}), $a=k_{app}$, which in turn can be defined as:

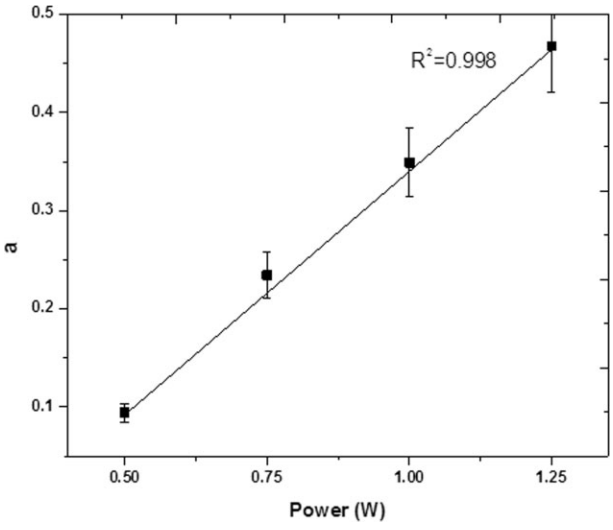

Figure 5. Parameter a as function of power.

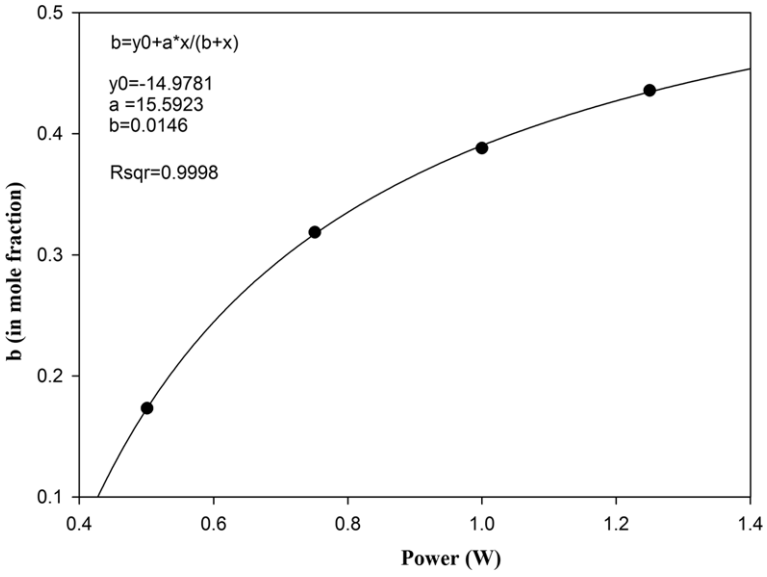

Figure 6. Parameter b as function of power.

$$k_{app} = k\,\eta e \quad (11)$$

$$\eta e = a\,P \quad (12)$$

where P is the power (W), a is a constant, k is the reaction rate constant, and ηe is the concentration of electrons that is linearly proportional to the power. So, the reaction rate can be written as:

$$-R = \frac{aPkC_{H_2S}}{b+C_{H_2S}} \quad (13)$$

Finally, by using the developed model, the reaction rate can be plotted as a function of the inlet concentration as presented in Fig. 7. The behavior of the reaction rate seems to be in line

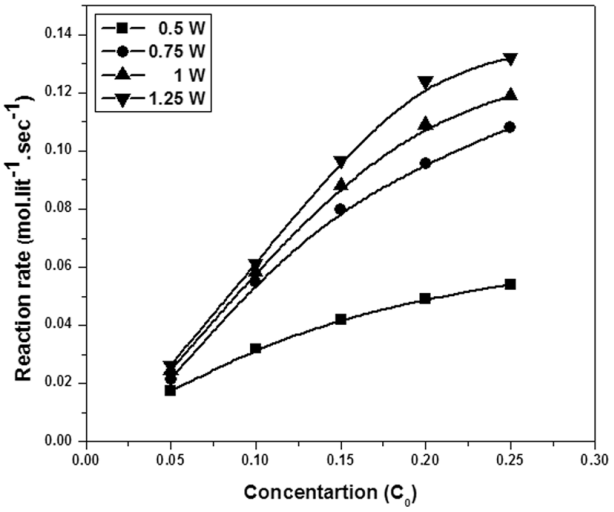

Figure 7. Reaction rate model to fit to the experimental points, $X=f(H_2S)$.

with the mechanism of H_2S decomposition that has been proposed in the previous section.

In the case of low input power, one may see that the amount of electrons capable of exciting the bulk molecules is very small and the number of excited Ar molecules is much lower than the amount of H_2S molecules. Under these conditions, the reaction rate depends only on the number of excited molecules or, in other words, on the power and not on the concentration of H_2S, hence the reaction order approaches zero. In the case of high input power, the number of excited Ar molecules may dominate the number of H_2S molecules in the bulk and the reaction becomes first order with respect to H_2S concentration.

In the case of high H_2S inlet concentrations, the direct electron collision with H_2S becomes the dominant reaction. The reaction order is close to zero as the number of H_2S molecules always remains higher than the number of excited Ar molecules. Also, at high H_2S concentration, H_2S molecules may reduce the discharge current in the reactor by capturing electrons as it is a more electronegative gas than Ar. In general, this effect is more pronounced for high H_2S concentrations, i.e., energy losses will be more at higher H_2S concentration. As a result, the electron concentration during discharge may be reduced, which may be due to the high electron affinity of hydrogen sulfide, hence leads to lower conversion. The excitation of Ar by electron collisions may be considered as the rate-limiting step at low input concentrations and high powers that may lead to first-order kinetic behavior, whereas high input concentrations and low powers may drive the reaction to zero order.

4 Conclusions

The decomposition of H_2S into its constituent elements hydrogen and sulfur has been evaluated in an NTP-DBD reactor. The kinetic study was performed to relate a reaction rate to H_2S concentration and power. A reaction rate model for H_2S decomposition was developed based on the Michaelis-Menten or Langmuir Hinshelwood model which confirmed the observation that the reaction order approaches zero with the increasing inlet concentration. The reaction rate was related to H_2S concentration and the power was a hyperbolic function.

Acknowledgment

This work was financially supported by the Ministry of New and Renewable Energy (MNRE), New Delhi, India.

The authors have declared no conflict of interest.

Symbols used

a, b	[–]	Michaelis-Menten kinetic model parameters
C_0	[vol %]	H_2S input concentration (also in units of mole fraction)
k_{app}	[–]	apparent rate constant
P	[W]	power
Q	[C]	charge
R	[mol $L^{-1}s^{-1}$]	reaction rate
X	[%]	conversion

Greek letters

α	[–]	constant
ηe	[–]	concentration of electrons
τ	[s]	residence time

References

[1] J. S. Eow, *Environ. Prog.* **2002**, *21 (3)*, 143.
[2] H. Ludewig, B. Haase, U. Fritsching, *Chem. Eng. Technol.* **2010**, *33 (1)*, 145.
[3] H. H. Kim, *Plasma Processes Polym.* **2004**, *1 (2)*, 91.
[4] U. Kogelschatz, *Plasma Chem. Plasma Process.* **2003**, *23 (1)*, 1.
[5] W. J. D. Escher, *Appl. Energy* **1994**, *47 (2–3)*, 201.
[6] V. E. Kaloidas, *Ph. D. Thesis*, National Technical University of Athens, Greece **1988**.
[7] V. E. Kaloidas, N. G. Papayannakos, *Chem. Eng. Sci.* **1989**, *44 (11)*, 2493.
[8] V. E. Kaloidas, N. G. Papayannakos, *Ind. Eng. Chem. Res.* **1991**, *30 (2)*, 345.
[9] N. I. Dowling, P. D. Clark, *Ind. Eng. Chem. Res.* **1999**, *38 (4)*, 1369.
[10] D. Woiki, P. Roth, *J. Phys. Chem.* **1994**, *98 (49)*, 12958.
[11] K. Karan, A. K. Mehrotra, A. B. Leo, *AIChE J.* **1999**, *45 (2)*, 383.
[12] J. E. Nicholas, C. A. Amodio, M. J. Baker, *J. Chem. Soc., Faraday Trans. 1* **1979**, *75*, 1868.
[13] G. B. Zhao, S. John, J. J. Zhang, J. C. Hamann, S. S. Muknahallipatna, S. Legowski, J. F. Ackerman, M. D. Argyle, *Chem. Eng. Sci.* **2007**, *62 (8)*, 2216.
[14] E. L. Reddy, V. M. Biju, C. Subrahmanyam, *Int. J. Hydrogen Energy* **2012**, *37 (3)*, 2204.
[15] C. Subrahmanyam, M. Magureanu, L. Kiwi-Minsker, A. Renken, *Appl. Catal., B* **2006**, *65 (1–2)*, 150.
[16] C. Subrahmanyam, M. Magureanu, L. Kiwi-Minsker, A. Renken, *Appl. Catal., B* **2006**, *65 (1–2)*, 157.
[17] M. Kraus, B. Eliasson, U. Kogelschatz, A. Wokaun, *Phys. Chem. Chem. Phys.* **2001**, *3 (3)*, 294.
[18] M. Magureanu, N. B. Mandache, V. I. Parvulescu, C. Subrahmanyam, A. Renken, L. Kiwi-Minsker, *Appl. Catal., B* **2007**, *74 (3–4)*, 270.
[19] E. Linga Reddy, J. Karuppiah, V. M. Biju, C. Subrahmanyam, *Int. J. Energy Res.* **2012**. DOI: 10.1002/er.2924
[20] G. B. Zhao, M. D. Argyle, M. Radosz, *J. Appl. Phys.* **2006**, *99 (11)*, 113302.

